3D Objects Indexing Using Spherical Harmonic for Optimum Measurement Similarity

S. Hellam, Y. Oulahrir, F. El Mounchid, A. Sadiq, S. Mbarki

Abstract—In this paper, we propose a method for three-dimensional (3-D)-model indexing based on defining a new descriptor, which we call new descriptor using spherical harmonics. The purpose of the method is to minimize, the processing time on the database of objects models and the searching time of similar objects to request object.

Firstly we start by defining the new descriptor using a new division of 3-D object in a sphere. Then we define a new distance which will be used in the search for similar objects in the database.

Keywords—3D indexation, spherical harmonic, similarity of 3D objects.

I. Introduction

THE goal of the 3D indexing is to describe compactly a 3D object shape. The objective is firstly the shape recognition in very large databases. To do this, shape descriptors are used to obtain vectors features or 3D objects signatures that serve keys in objects retrieval.

Just like the Fourier basis represents an important tool for evaluation of convolutions in a one- or two dimensional spaces, the spherical harmonic basis is a similar tool but defined on the surface of a sphere. Spherical harmonics have already been used in the field of computer graphics [1]-[4]. But spherical harmonics have just recently become feasible to be used in real time computer graphics. Spherical harmonics is used to compute graphics to a certain degree [5].

In this work we propose a new descriptor based on a random distribution's centroid in which we use spherical harmonics calculated in spherical triangles. The new distance which is defined in this paper is used for measuring similarity -between request objects and objects models in database.

II. State of Art

In order to solve the problem of data treatment: storing, editing and manipulating, very powerful programs was developed for importing the data files and exporting them in well-standardized formats, like IGES, DXF for CAD applications and VRML for visualization [6].

To evaluate the efficiency of the descriptor, the properties of invariance are required to eliminate differences due to translation, rotation and magnification.

The literature provides a lot of various 3D shape descriptors, describing geometric as well as topological properties of 3D shapes: global shape descriptors [7], [8]; local descriptors [9]; graph based methods [10], [11]; geometric methods based on 2D views of 3D models [12], [13].

In the rest of their work, the team of Leipzig has also proposed to apply a Fourier transform on the sphere S_2 [13] by applying the proposed spherical harmonic.

Then, to overcome the problem of invariance to rotation, the Princeton team proposed to apply the spherical harmonic decomposition of spherical functions defined by the intersection of the surface of the 3D object with a set of concentric spheres [14].

The spherical harmonics method of Princeton's team gave better results in their database than their previous descriptor (distribution of D2 form). However, it is based on a 3D model voxelization; therefore, depends on the level of resolution of the voxelization, and resulting in a loss of detail in the description of the object.

That is why [13] proposes to apply the method directly on 3D meshes with new spherical functions. The results they obtained on their database with their method are less time consuming.

However, these results also show that the encoded information does not really make specific requests on shapes, the main limitation is the number of concentric spheres and the number of coefficients harmonics remaining may be too low. The authors choose in practice 32 concentric spheres and 16 harmonics per sphere. Thus, their descriptor has 32*16= 512 coefficients.

Different 3D shape description methods have been proposed in this research area. Teams [15] have realized a comparative study of 3D retrieval algorithms [14], [20]. Those algorithms can be clustered into two main families: 2D/3D approaches and 3D/3D approaches. The descriptor using 2D / 3D approaches, the description model is obtained through different 2D projections of the 3D shape, whereas for the descriptor using 3D/3D approaches, the description model is obtained from the 3D information directly extracted from the 3D shape [19], [21].

III. Spherical Harmonic Method

A. Invariant 3D Shape Descriptors

The properties of invariance are required to eliminate differences due to rotation, translation and magnification. To avoid of these dependencies, we shall normalize the models by

S. Hellam is with LABO LARIT, Faculty of Science, Ibn tofail University Morocco (phone: +212672498117; e-mail: hellamsaid@gmail.com).

Y. Oulahrir is with Office of Vocational Training and Job Promotion (phone: +212669790756; e-mail: oulahrir.ntic2@gmail.com).

F. El Mounchid is with the Ministry of Education (e-mail: elmounchid@yahoo.fr).

A. Sadiq and S. Mbarki are with IBN TOFAIL University (e-mail: sadiq.alim@gmail.com, mbarkisamir@hotmail.com).

World Academy of Science, Engineering and Technology
International Journal of Computer and Information Engineering
Vol:9, No:1, 2015

using the center of mass for translation, the root of the average square radius for scale and principal axis for rotation [7], [16].

B. Representation of Spherical Harmonics

The gradient in spherical coordinates is [17]:

$$\vec{\nabla} = \frac{\partial}{\partial\theta}\vec{e}_r + \frac{1}{r}\frac{\partial}{\partial\theta}\vec{e}_\theta + \frac{\partial}{\partial\varphi}\vec{e}_\varphi \tag{1}$$

The Laplacian of a function f:

$$\nabla^2 f = \frac{1}{r^2}\frac{\partial}{\partial r}\left(r^2\frac{\partial f}{\partial r}\right) + \frac{1}{r^2\sin\theta}\frac{\partial}{\partial\theta}\left(\sin(\theta)\frac{\partial f}{\partial\theta}\right) + \frac{1}{r^2\sin(\theta)}\frac{\partial^2 f}{\partial\varphi^2} \tag{2}$$

$$Y_l^m(\theta,\varphi) = \sqrt{\frac{2l+(l-m)!}{4\pi(l+m)!}}P_l^m(\cos(\theta))e^{im\varphi} \tag{3}$$

P_l^m is the Legendre polynomial associated of l degree and m order, θ varies between $[0,\pi]$ and φ varies between $[0,2\pi]$ [18] .

$$P_l^m(x) = \frac{(-1)^m}{2^l l!}(1-x^2)^{\frac{m}{2}}\frac{d^{l+m}}{dx^{l+m}}(x^2-1)^l \tag{4}$$

Spherical harmonic decomposition: $\{Y_l^m / m \in Z \ et \ l \in N\}$ Orthonormal basis in the Hilbert space L^2 (S^2) with S^2 unit sphere [19].

$$\int_0^{2\pi}\int_0^{\pi} Y_l^m(\theta,\varphi)\overline{Y}_{l'}^{m'}(\theta,\varphi)\sin(\theta)d\theta\,d\varphi = \delta_{ll'}\cdot\delta_{mm'} \tag{5}$$

δ_{ij} is Symbol of Kronecker, where:

$$\delta_{ij} = \begin{cases}1 & \text{if } i=j \\ 0 & \text{if } i \neq j\end{cases} \tag{6}$$

We have:

$$-\Delta Y_l^m(\theta,\varphi) = l(l+1)Y_l^m(\theta,\varphi) \tag{7}$$

and:

$$-i\frac{\partial}{\partial\varphi}Y_l^m = mY_l^m \tag{8}$$

The Graphical Representation:

Representative surfaces are bumpy spheres: bumps correspond to the parts where $Y_l^m(\theta,\varphi)$ positive, dips are corresponding to the parts where $Y_l^m(\theta,\varphi)$ is negative, θ and φ describe the interval $[0,\pi]$ and $[0,2\pi]$. $Y_l^m(\theta,\varphi)$ vanishes according l circles [18].

- m: circles along the meridian, an iso-longitude.
- ▧-m: circles in a parallel, an iso-latitude.

Spherical Harmonic Decomposition (S.H.D):

Let $f(\theta,\varphi)$ be a harmonic function defined on the closed interval $[-1,1]$ [19].

$$f(\theta,\varphi) = \sum_{l=0}^{\infty}\sum_{m=-l}^{l}C_{lm}Y_l^m(\theta,\varphi) \tag{9}$$

$C_{l,m}$ are the harmonic coefficients of order (▧, m)

Hermitian Scalar Product:

$$\langle f,g\rangle = \frac{1}{4\pi}\iint_{S^2}f^*g\sin(\theta)\,d\theta\,d\varphi \tag{10}$$

where f^* is the complex conjugate of f indeed:

$$C_{l,m} = \langle Y_l^m, f\rangle = (-1)^m\sqrt{\frac{2l+(l-m)!}{4\pi(l+m)!}}\int_0^{2\pi}\int_0^{\pi}P_l^m(\cos(\theta))e^{-im\varphi}\sin(\theta)\,d\theta\,d\varphi \tag{11}$$

We have:

$$C_{l,-m} = (-1)^m C_{l,m}^* \tag{12}$$

$C_{l,m}^*$: is the complex conjugate of $C_{l,m}$.

From (12), it is sufficient to calculate the coefficients $C_{l,m}$ for m positive, so that reduced half of the computation time. The dimension of the L^2 (S^2) space is $2l+1$. ξ: is the set of points which create the 3D object

The Indicator Function:

$$\chi(r,\theta,\varphi) = \begin{cases}1 & \text{if } M \in \xi_S \\ 0 & \text{if } M \notin \xi_S\end{cases} \tag{13}$$

where ξ_s is the set of points belonging to the object and the sphere (S^2) with radius r. Thus: $\zeta_s = \zeta \cap (S^2)$

We calculate the coefficients of the spherical harmonics for different cases of m:

- $m = 0$
- $0 < m < l$
- $m = l$

We use a numerical method Simpson and we subsequently construct the matrix H given by the following expression:

$$H = \begin{bmatrix} C_{l,-l}^1 & \cdots & C_{l,-l+j}^1 & \cdots & C_{l,l}^1 \\ \vdots & \ddots & \vdots & \cdots & \vdots \\ C_{l,-l}^i & \cdots & C_{l,-l+j}^i & \cdots & C_{l,l}^i \\ \vdots & \vdots & \vdots & \ddots & \vdots \\ C_{l,-l}^N & \cdots & C_{l,-l+j}^N & \cdots & C_{l,l}^N \end{bmatrix}$$

This matrix is represented by a 2l +1 rows and N columns, where N is the number of points which represents the 3D object.

Each row R_k characterize the point P_k by the $2l+1$ coefficients of spherical harmonic $C_{l,m}^k$, where $1 \leq k \leq N$ and $-l \leq m \leq l$.

In each column C_m we calculate the different coefficients $C_{l,m}^k$ for all points defining the object.

World Academy of Science, Engineering and Technology
International Journal of Computer and Information Engineering
Vol:9, No:1, 2015

C. Measurement of Similarity Based On New Distance Using Spherical Harmonic Coefficients

We define for same value l the coefficient F_{ij} :

$$F_{l,i} = \max_{1 \leq k \leq N_i} \frac{\sum_{m=-l}^{l}\left|C_{l,m}^{k}\right|}{2l+1} \quad (14)$$

Where i indicate the object O_i and N_i is the number of points in O_i.

The role of the factor $\frac{1}{2l+1}$ is to calculate the average of the sum of coefficients values $\left|C_{l,m}^{k}\right|$ for each point.

To calculate the similarity between two objects O_i and O_j, we use the similarity distance defined by the following expression:

$$S_d = \frac{\left|F_{l,i}^{\frac{1}{N_i}} - F_{l,j}^{\frac{1}{N_j}}\right|}{\min(N_i, N_j)} \quad (15)$$

We use the power $\frac{1}{N_i}$ and the $\min(N_i, N_j)$ in the formula of the similarity distance in order to mitigate the effect of varying the number of points in the search for similar objects.

Special Case:

When N_j is positive infinity the object O_j becomes opaque (O_j is dominant to O_i). Then in this case, S_d is defined by the following expression:

$$S_d = S_d^{+\infty} = \frac{\left|F_{l,i}^{\frac{1}{N_i}} - 1\right|}{N_i} \quad (16)$$

S_i only depends on the object O_i.

IV. EXPERIMENTS AND RESULTS

Experience 1:

For testing the new distance of similarity indicated in (15) for 3D objects, we have chosen three classes of objects: cars, planes and rabbits as have been shown in Fig. 1.

In order to test the distance of similarity chosen, we compare an object to the other objects in the same class.

Tables I-III show the number of points for each object per class type.
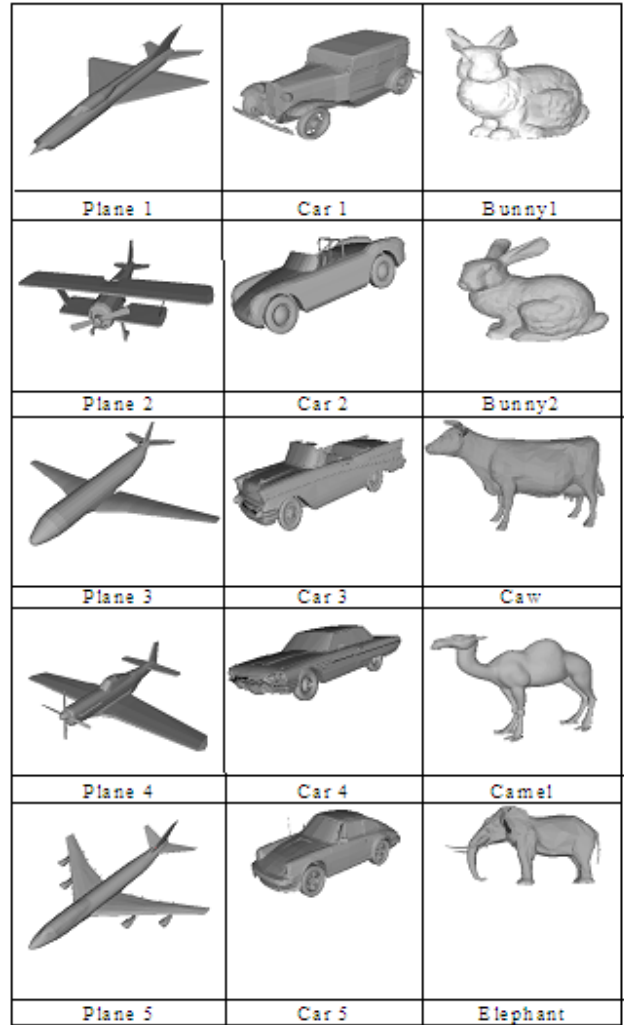

Fig. 1 Three classes of objects: cars, planes and animals

TABLE I
NUMBER OF POINTS FOR EACH OBJECT IN THE CARS CLASS

Object	Number of Points
Car 1	10466
Car 2	30307
Car 3	18472
Car 4	7474
Car 5	6318

TABLE II
NUMBER OF POINTS FOR EACH OBJECT IN THE PLANES CLASS

Object	Number of Points
Plane 1	971
Plane 2	3361
Plane 3	1401
Plane 4	1606
Plane 5	5188

TABLE III
NUMBER OF POINTS FOR EACH OBJECT IN THE ANIMALS CLASS

Object	Number of Points
Bunny 1	1494
Bunny 2	26002
Cow	2904
Camel	9770
Elephant	10589

World Academy of Science, Engineering and Technology
International Journal of Computer and Information Engineering
Vol:9, No:1, 2015

Table IV shows a sample of the values of the S_d distance calculated between Plane3 and other aircraft from the same class for a tart values of *l* between 1 and 35.

TABLE IV
MEASUREMENT OF SIMILARITY BETWEEN THE PLANE 3 AND THE OTHER PLANES IN THE SAME CLASS

Value l	Plane3-Plane1	Plane3-Plane4	Plane3-Plane5	Plane3-Plane2
1	9.936E-001	9.945E-001	9.9739E-001	9.9591E-001
2	9.940E-001	9.948E-001	9.9749E-001	9.9610E-001
3	9.941E-001	9.948E-001	9.9753E-001	9.9620E-001
10	9.948E-001	9.953E-001	9.9776E-001	9.9659E-001
11	9.949E-001	9.955E-001	9.9781E-001	9.9666E-001
12	9.950E-001	9.956E-001	9.9785E-001	9.9674E-001
20	9.962E-001	9.964E-001	9.9825E-001	9.9741E-001
21	9.963E-001	9.965E-001	9.9830E-001	9.9749E-001
22	9.964E-001	9.966E-001	9.9835E-001	9.9757E-001
34	9.983E-001	9.981E-001	9.9896E-001	9.9864E-001
35	9.984E-001	9.983E-001	9.9902E-001	9.9874E-001

For testing the similarity distance, we draw the graph of a function S_d depending on the parameter l.
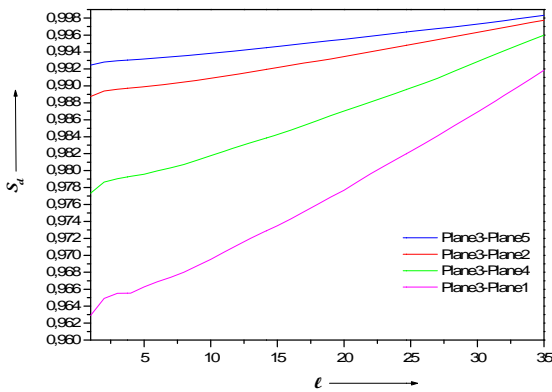

Fig. 2 Measurement of similarity between plane3 and other planes in the class

Fig. 2 shows that plane5 is most similar to the plane3 relative to other aircraft.
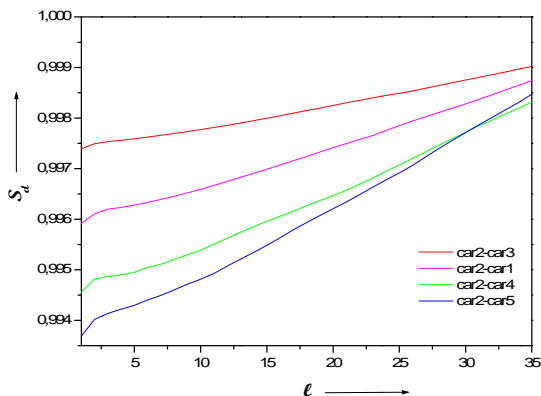

Fig. 3 Measurement of similarity between car2 and others cars in the class

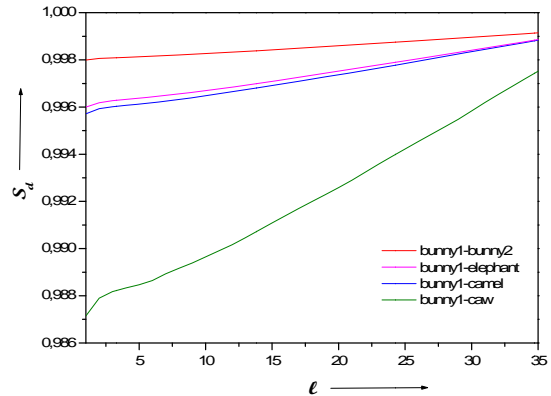Fig. 3 shows that Car 3 is most similar to the Car 2 relative to other cars.

Fig. 4 Measurement of similarity between bunny1 and other animals in the class

Fig. 4 shows that bunny 2 is most similar to the bunny 1 relative to other bunnies the distance of similarity between bunny 1 and cow.

All figures S_d in function of l notes that objects are more similar if similarity distance is more important. This resemblance becomes very important when l increases because you see more detail the 3D object. For l= 35, 71 coefficients are calculated for each point, more spherical harmonics which increases the symmetry for the two objects.

The distance $S_d = 0$ when comparing an object to itself.

Experience 2:

In the next step we test our new descriptor on the same object with different points as shown in Fig. 5:
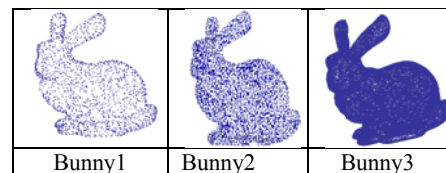

Fig. 5 Objects of the same class with different number of points.

TABLE V
NUMBER OF POINTS FOR EACH OBJECT BUNNY

Object	Number of Points
Bunny 1	1494
Bunny 2	26002
Bunny 3	34834

Fig. 6 shows that bunny 3 and 2 is most similar to the bunny 1 relative to a cow and a camel. This result proves that our similarity distance provides highly reliable measurement, but not at 100%.

Fig. 6 shows the existence of a low error due to augmentation of number of points for the same object. That's why we define a coefficient of relative error δ_r as shown in:

World Academy of Science, Engineering and Technology
International Journal of Computer and Information Engineering
Vol:9, No:1, 2015

$$\delta_r = \frac{\left|S_{d,1} - S_{d,2}\right|}{\min(S_{d,1}, S_{d,2})} \times 100 \qquad (17)$$
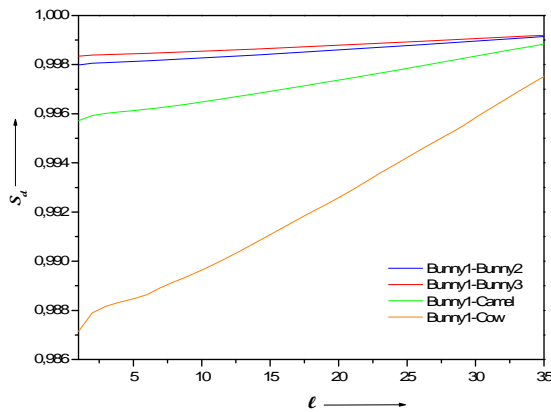

Fig. 6 Measurement of similarity between bunny1 and others bunnies, with a camel and a cow
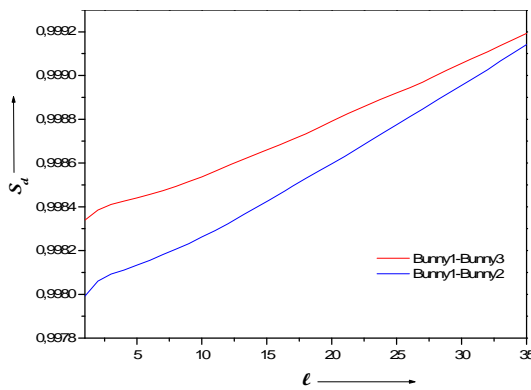

Fig. 7 Measurement of similarity between bunny1 and bunnies 2 and 3

Fig. 7 shows that the S_d values almost the same, but did not stop to give the variations of the two curves and gives the relative error for the two curves shown in Table VI.

TABLE VI
MEASUREMENT ERROR BETWEEN THE S_d (BUNNY1-BUNNY2) AND S_d (BUNNY1-BUNNY3)

l	S_{dl2}	S_{dl3}	δ_r
2	9,98060E-01	9,98385E-01	3,26036E-02
5	9,98134E-01	9,98441E-01	3,07810E-02
10	9,98262E-01	9,98537E-01	2,74928E-02
15	9,98425E-01	9,98660E-01	2,34753E-02
20	9,98597E-01	9,98791E-01	1,94376E-02
25	9,98776E-01	9,98921E-01	1,45304E-02
30	9,98955E-01	9,99056E-01	1,00506E-02
35	9,99142E-01	9,99193E-01	5,08861E-03

We note, in Table VI that the relative error decreases as increases l.

V. CONCLUSION AND FUTURE WORK

In this paper, we have presented a new method for Three-dimensional object indexing. To this end, we have benefit from advantages of spherical harmonic. First, we calculated the coefficients of spherical harmonics numerically. Next, we defined a new similarity distance and we justified our choice. In the end, we tested our distance on three different classes of objects: planes, cars and animals. Our results proof the efficiency of our similarity distance. But we hope, in the future work, to improve our results and minimize the relative error. Currently, we search to calculate directly the coefficients of spherical harmonics.

REFERENCES

[1] B.Cabral, N. Max and R. Springmeyer. Bidirectional Reflection Functions from Surface Bump Maps SIGGRAPH 273-281, 1987
[2] Volker Schönefeld, Spherical Harmonics,1st July 2005
[3] Gerig, G. Styner, M. Jones, D., Weinberger, D. Lieberman, J., 2001. Shape analysis of brain ventricles using spharm. In: MMBIA , pp. 171-178.
[4] B.K.P Horn. Extended Gaussian Images. Proc. of the IEEE, 72(12):1671–1686, dec. 1984.
[5] http://scienceblogs.de/mathlog/2011/09/30/topologie-von-flachen-clxxxvii/
[6] S.B. Kang and K. Ikeuchi. The complex EGI: a new representation for 3D pose determination. IEEE Trans. on Pattern Analysis and Machine Intelligence, 16(3):249–258, March 1994.21, hal-00538470, version 1 - 22 Nov 2010
[7] Brecbuhler, Ch., Gerig, G., Kuhler, O., 1995. Parameterization of closed surfaces for 3D shape description. Computer Image and Vision Understanding 61 (2), 154-170.
[8] R. Ohbuchi, T.Minamitani, and T .Takei. Shape-similarity search of 3D models by using enhanced shape functions. In Int. J. of Computer Applications inTechnology (IJCAT), 23(3/4/5):70-85, 2005.
[9] P. Papadakis, I. Pratikakis, S. Perantonis, and T. Theoharis. Efficient 3D Shape Matching and Retrieval using a Concrete Radialized Spherical Projection Representation. Pattern Recognition Journal, 40(9):2437–2452, Sept. 2007.
[10] M. Ben-Chen and C. Gostman. Characterizing Shape Using Confor- mal Factors. In Eurographics Workshop on 3D Object Retrieval, Crete, Greece., April 2008.
[11] T. Tung and F. Schmitt. The augmented multiresolutionReeb graph approach for content-based retrieval of 3D shapes. International Journal of Shape Modeling (IJSM), 11(1):91–120, June 2005.
[12] S. Biasotti, D. Giorgi, M. Spagnuolo, and B. Falcidieno. Reeb graphs for shape analysis and applications. Theoretical Computer Science, 392 (1-3):5–22, 2008.22 hal-00538470, version 1 - 22 Nov 2010
[13] D.V. Vranic. 3D Model Retrieval. PhD thesis, University of Leipzig, 2004.
[14] M. Kazhdan, B. Chazelle, D. Dobkin, T. Funkhouser, and S. Rusinkiewicz. A Reflective Symmetry Descriptor for 3D Models. Al- gorithmica, 38(1):201–225, 2003.
[15] J.W.H. Tangelder and R.C. Veltkamp, "A survey of content based 3D shape retrieval methods," Multimedia Tools and Applications, vol. 39, no. 3, pp. 441–471, Sept. 2008.
[16] Gerig, G. Styner, M. Jones, D., Weinberger, D. Lieberman, J., 2001. Shape analysis of brain ventricles using spharm. In: MMBIA , pp. 171-178.
[17] René Lagrange, Polynômes et fonctions de Legendre coll. Mémorial des sciences mathématiques, n° 97, Gauthier-Villars, 1939.
[18] W. E. Byerly. Spherical Harmonics, chapter 6, pages 195-218.New York: Dover, 1959. An elementary treatise on fourier's series and spherical, cylindrical, and ellipsoidal harmonics, with applications to problems in mathematical physics.
[19] M. Mousa, R. Chaine, and S. Akkouche. Frequency-based representation of 3d models using spherical harmonics. In WSCG'06 : Proceedings of the 14th International Conference in Central Europe on Computer Graphics, Visualization and Computer Vision, volume 14, pages 193–200, Plzen, Czech Republic, January 30 - February 3 2006.
[20] T. Zaharia and F. Prêteux, "3D versus 2D/3D shape descriptors: A comparative study," in SPIE Conf. on Image Processing: Algorithms and Systems III - IS & T/ SPIE Symposium on Electronic Imaging, Science and Technology '03, San Jose, CA, Jan. 2004, vol. 5298

[21] M. Chaouch and A. Verroust-Blondet, "A new descriptor for 2D depth image indexing and 3D model retrieval," in Proc. ICIP'07, vol. 6, 2007, pp. 373–376.